

Cavity locking with spatial modulation of optical phase front for laser stabilization*

Sheng Feng,[†] Songqing You,[‡] Peng Yang, Fenglei Zhang, and Yunlong Sun
*School of Electrical and Electronic Information Engineering,
 Hubei Polytechnic University, Huangshi, Hubei 435003, P.R. China*

Boya Xie
*Hubei Key Laboratory of Modern Manufacturing Quantity Engineering,
 School of Mechanical Engineering, Hubei University of Technology, Wuhan, Hubei 430068, China.*
 (Dated: July 13, 2022)

We study optical cavity locking for laser stabilization through spatial modulation of the phase front of a light beam. A theoretical description of the underlying principle is developed for this method and special attention is paid to residual amplitude modulation (RAM) caused by experimental imperfections, especially the manufacture errors of the spatial phase modulator. The studied locking method owns the common advantages of the Pound-Drever-Hall method and the tilt-locking one, and it can provide a more artful way to eliminate RAM noise in phase modulation for the ultimate stability of lasers. In situations where cost and portability are a practical issue, the studied method allows one to realize compact laser stabilization systems locked to Fabry-Pérot cavities without use of expensive bulky devices, such as signal generators and electro-optic modulators.

Ultra-stable lasers with high-spectral purity play an essential role in a variety of advanced research fields, such as optical atomic clocks [1–3], tests of relativity [4, 5], gravitational wave detectors [6], and photonic microwave synthesizers [7]. State-of-the-art stable lasers locked to high-finesse Fabry Pérot (FP) cavities delivering single-mode electromagnetic waves have been realized with integral linewidths below 1 Hz [8, 9]. Another research direction of relevance is to construct portable stable laser systems [10] towards applications wherein robustness and integration are primary concerns, with a 20-ms stability of 10^{-13} already reported [11]. Despite several locking schemes of potential interest [12–16], most of these performance demonstrations have been accomplished by use of the standard Pound-Drever-Hall (PDH) one [17] in which the phase front of the optical carrier undergoes temporal modulation that generates radio frequency (r.f.) sidebands.

A well-known issue with the PDH modulation technique is residual amplitude modulation (RAM) that arises when the r.f. modulation sidebands are unequal in magnitude, not exactly out of phase, or both. RAM couples frequency offset noise to the servo error signal and thereby aggravates the laser frequency instability. A few RAM reduction schemes [18–21] have been implemented with the most remarkable one demonstrated recently [22] that utilized an active servo loop involving both DC electric field and temperature corrections applied to the phase modulator. RAM control on the 10^{-6} level was reported with a RAM-induced frequency instability comparable to or lower than thermal noise limit [22].

Instead of using *temporal* modulation as the PDH method does [17], we explore in this work *spatial* modulation of the optical phase front of the carrier for FP cavity locking. Aside from its own merit of fundamental interest, the studied cavity locking method provides handy ways for RAM reduction; moreover, it has the common advantages of the PDH method and the tilt-locking one the later of which nonetheless utilizes travelling-wave cavities for laser stabilization [23]. In comparison with the PDH one, the studied method can provide larger error signals for the servo loop and may eliminate the need of electro-optic modulators (EOM's) and signal generators that are expensive, bulky, and otherwise necessary for temporal phase modulation, which is beneficiary to low-cost portable laser stabilization systems locked to FP cavities [10, 11].

In what follows, let describe the principle underlying the studied cavity locking method through spatial modulation of optical phase front. For simplicity without loss of generality, let consider a collimated laser beam in a Gaussian mode, $E_1(\vec{r}, t)$, that is coupled into an FP cavity through a focal lens (Fig. 1). A transparent optical element, namely a spatio-optic modulator (SOM), is inserted into the incident light beam before the lens such that the phase front of the beam undergoes spatial modulation. The spatially modulated light field $E_m(\vec{r}, t)$ is described as,

$$E_m(\vec{r}, t) = E_1(\vec{r}, t)U(\vec{r}) = E_1(\vec{r}, t)e^{i\varphi(\vec{r})}, \quad (1)$$

wherein $U(\vec{r})$ is the SOM modulation function, and the vector \vec{r} represents the two-dimensional coordinates in the plane perpendicular to the propagation axis of the light beam. Unity transmittance is assumed for the SOM and $\varphi(\vec{r})$ is the spatial distribution of the change to the light field phase front caused by the SOM.

To get an insight into the cavity locking method, let assume $|\varphi(\vec{r})| \ll 1$ for the moment. Under this assump-

* A footnote to the article title

[†] fensf2a@hust.edu.cn

[‡] Also at Hubei Key Laboratory of Modern Manufacturing Quantity Engineering, School of Mechanical Engineering, Hubei University of Technology, Wuhan, Hubei 430068, China.

tion, the modulated light field $E_m(\vec{r}, t)$ reads

$$E_m(\vec{r}, t) = E_i(\vec{r}, t) + i\varphi(\vec{r})E_i(\vec{r}, t), \quad (2)$$

from which it follows that the modulated light field becomes a superposition of the incident light field, $E_i(\vec{r}, t)$, and another effective field, $E_e(\vec{r}, t) \equiv i\varphi(\vec{r})E_i(\vec{r}, t)$, as a consequence of spatial modulation. For the purpose of this work, the SOM may be designed for $\varphi(\vec{r})$ to satisfy

$$\iint d\vec{r} E_i^*(\vec{r}, t) E_e(\vec{r}, t) = \iint d\vec{r} \varphi(\vec{r}) |E_i(\vec{r}, t)|^2 = 0, \quad (3)$$

in which the integral area covers the whole cross section of the incident beam. In other words, the spatial mode of the effective field, $E_e(\vec{r}, t)$, is orthogonal to that of the incident field, $E_i(\vec{r}, t)$, and hence the two fields may not simultaneously resonate inside a narrow-linewidth optical cavity due to their spatial mode orthogonality [24].

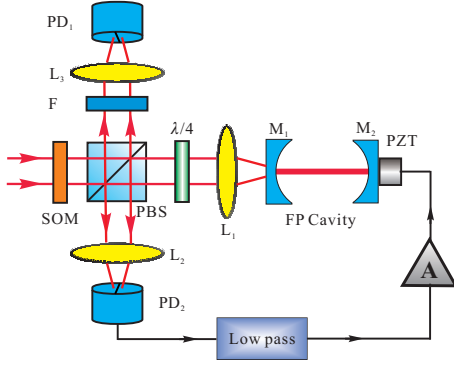


FIG. 1. (color online) Schematics for cavity locking by spatial modulation of optical phase front. SOM: Spatio-optic modulator. PBS: Polarizing beam-splitter. $\lambda/4$: Quarter wave plate. $L_{1,2,3}$: Focal lens coupling the incident light into the cavity. $M_{1,2}$: Cavity mirrors. PZT: Piezo-electrical transducer. $L_{2,3}$: Imaging lenses used to map the SOM images to the corresponding photo-detectors. $PD_{1,2}$: Dual-quadrant photo-detectors. F: An optional optical element used to tailor the spatial mode amplitudes of the light field received by PD_1 for RAM cancellation.

Now let suppose that the incident field $E_i(\vec{r}, t)$ is near resonance in the FP cavity of Fig. 1, and that the cavity linewidth is narrow enough so that the effective field $E_e(\vec{r}, t)$ is far-off resonance. Then after reflection from the cavity, the modulated light field becomes [12]

$$\begin{aligned} E_r(\vec{r}, t) &= \left\{ \sqrt{R_1} [1 + i\varphi(\vec{r})] - \frac{T_1}{\sqrt{R_1}} \frac{e^{i\delta} \sqrt{R}}{1 - e^{i\delta} \sqrt{R}} \right\} E_i(\vec{r}, t) \\ &= [\chi e^{i\theta} + i\varphi(\vec{r})] \sqrt{R_1} E_i(\vec{r}, t), \end{aligned} \quad (4)$$

in which

$$\chi e^{i\theta} \equiv 1 - \frac{T_1}{R_1} \frac{e^{i\delta} \sqrt{R}}{1 - e^{i\delta} \sqrt{R}}, \quad (5)$$

and R_1, T_1 are respectively the reflectivity and transmissivity of the cavity entrance mirror M_1 , $R \equiv R_1 R_2$ (R_2

the reflectivity of the other cavity mirror M_2), and δ stands for the round trip phase delay of the light field inside the cavity.

In what follows, we will show how to exploit an optical element of spatial modulation, i.e. an SOM, to implement cavity locking based on Eq. (4). Given that the incident light field $E_i(\vec{r}, t)$ is in a Gaussian mode which is symmetric with respect to the light propagation axis,

$$E_i(\vec{r}, t) = E_i(-\vec{r}, t), \quad (6)$$

one may utilize an SOM with a spatial modulation function that introduces an anti-symmetric phase change to the incident beam around its axis,

$$\varphi(\vec{r}) = -\varphi(-\vec{r}). \quad (7)$$

From Eqs. (6) and (7) it immediately follows that Eq. (3) holds true and, hence, so does Eq. (4). An example of a designed SOM satisfying Eq. (7) is illustrated in Fig. 2 and the phase front change $\varphi(\vec{r})$ of the light field due to the spatial modulation reads

$$\varphi(\vec{r}) = \begin{cases} \pm\varphi_0 & |\vec{r} \mp r_0| < r_0 \\ 0 & \text{otherwise} \end{cases}, \quad (8)$$

in which $\pm\varphi_0$ are constant modulation-induced phase changes in the corresponding areas, $S_{1,2}$, which are circular here centered at the points of $(\pm r_0, 0)$ respectively with the same radius of r_0 .

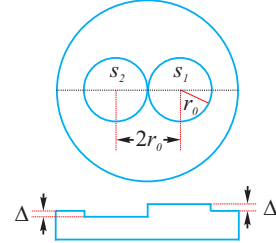


FIG. 2. (color online) An example of a designed SOM for cavity locking. $\Delta \equiv (\varphi_0/2\pi) \cdot \lambda/(n-1)$ with λ being the wavelength of the light beam and n the refractive index of the SOM material). (Top): Front view of the SOM. (Bottom): The SOM surface profile along the dash line as indicated on the top.

Next we will show how an error signal may be obtained in the cavity locking method. To this end, one may use a dual-quadrant photo-detector to receive the light beam reflected from the cavity. An optical imaging system is utilized to project the image of the SOM onto the photo-detector, with each quadrant aligned with respect to each of the circles, $S_{1,2}$, on the SOM. The output photo-electric currents from the two quadrants are subtracted to produce an error signal $\varepsilon(\delta)$ as described by,

$$\varepsilon(\delta) = \iint_{S_1} d\vec{r} |E_r(\vec{r}, t)|^2 - \iint_{S_2} d\vec{r} |E_r(\vec{r}, t)|^2. \quad (9)$$

To make it clearer, one may plug Eqs. (4) and (8) into Eq. (9), leading to

$$\begin{aligned}\varepsilon(\delta) &= \iint_{S_1} d\vec{r} R_1 |(\chi e^{i\theta} + i\varphi_0) E_1(\vec{r}, t)|^2 \\ &\quad - \iint_{S_2} d\vec{r} R_1 |(\chi e^{i\theta} - i\varphi_0) E_1(\vec{r}, t)|^2 \\ &= 4R_1 I_0 \varphi_0 \chi \sin \theta \\ &= 4R_1 I_0 \varphi_0 \operatorname{Im} \left(1 - \frac{T_1}{R_1} \frac{e^{i\delta} \sqrt{R}}{1 - e^{i\delta} \sqrt{R}} \right), \quad (10)\end{aligned}$$

in which $\operatorname{Im}(\cdot)$ stands for the imaginary part of a complex number and one has invoked Eq. (6) from which it follows that $\iint_{S_1} d\vec{r} |E_1(\vec{r}, t)|^2 = \iint_{S_2} d\vec{r} |E_1(\vec{r}, t)|^2 \equiv I_0$. The error signal for cavity locking varies as a function of cavity detuning δ from its peak resonance according to Eq. (10).

In what follows, let turn to the RAM problem associated with the studied cavity locking method due to SOM manufacture errors. Specifically, the anti-symmetry given by Eq. (7) may be broken to some extent in practice resulting from the difference between the areas, optical transmissivities, modulation depths of S_1 and S_2 ; the SOM symmetry breaking, together with unexpected input beam drifting, unbalanced quantum efficiencies and unequal gains of the two quadrants of the photo-detector, will invalidate the assumptions of both Eq. (8) and $\iint_{S_1} d\vec{r} |E_1(\vec{r}, t)|^2 = \iint_{S_2} d\vec{r} |E_1(\vec{r}, t)|^2$, causing RAM noises in the error signal. One should note that both the real RAM noises and RAM-like noises are referred to as ‘‘RAM noises’’ in this work when they cannot be distinguished in experiment.

To account for these effects in theory, one may define different phase modulations $\varphi_{1,2}$ for each of the two circular areas $S_{1,2}$ respectively with radii $r_{1,2} < r_0$,

$$\varphi(\vec{r}) = \begin{cases} \varphi_1 & |\vec{r} - r_0| < r_1 \\ 0 & \text{otherwise} \\ \varphi_2 & |\vec{r} + r_0| < r_2 \end{cases}, \quad (11)$$

and photo-currents $I_{1,2}$,

$$I_1 \equiv G_1 \iint_{S_1} d\vec{r} |E_1(\vec{r}, t)|^2, \quad I_2 \equiv G_2 \iint_{S_2} d\vec{r} |E_1(\vec{r}, t)|^2. \quad (12)$$

Here the normalized coefficients $G_{1,2}$ account for all the effects resulting from the differences in the optical transmissivities of the areas $S_{1,2}$, beam drifting, the gains and quantum efficiencies of the two detector quadrants.

With Eqs. (4), (11), and (12), the error signal becomes

$$\begin{aligned}\varepsilon(\delta) &= G_1 \iint_{S_1} d\vec{r} R_1 |(\chi e^{i\theta} + i\varphi_1) E_1(\vec{r}, t)|^2 \\ &\quad - G_2 \iint_{S_2} d\vec{r} R_1 |(\chi e^{i\theta} - i\varphi_2) E_1(\vec{r}, t)|^2 \\ &= 4R_1 (\bar{I} \bar{\varphi} + \Delta I \Delta \varphi) \operatorname{Im} \left(1 - \frac{T_1}{R_1} \frac{e^{i\delta} \sqrt{R}}{1 - e^{i\delta} \sqrt{R}} \right) \\ &\quad + 2R_1 [2\bar{I} \bar{\varphi} \Delta \varphi + \Delta I (\chi^2 + \bar{\varphi}^2 + (\Delta \varphi)^2)], \quad (13)\end{aligned}$$

in which $\bar{I} = (I_1 + I_2)/2$, $\Delta I = (I_1 - I_2)/2$, $\bar{\varphi} = (\varphi_1 + \varphi_2)/2$, and $\Delta \varphi = (\varphi_1 - \varphi_2)/2$. The first term on the right hand side of Eq. (13) is the error signal required for cavity locking, whereas the second term describes RAM in the studied scheme that introduces frequency offset noise into the servo error signal leading to degradation of the laser frequency stability.

To get rid of RAM noises in the scheme, one may adjust the coefficients $G_{1,2}$ to change the value of $\Delta I = (I_1 - I_2)/2$ according to Eq. (12) such that

$$\Delta I = -\frac{2\bar{I} \bar{\varphi} \Delta \varphi}{\chi^2 + \bar{\varphi}^2 + (\Delta \varphi)^2}, \quad (14)$$

which guarantees zero RAM, i.e., the second term in Eq. (13) becomes null. Equality (14) can be realized without much difficulty in practice by varying the optical transmissivities of the areas $S_{1,2}$ on the SOM and/or the gains of the two quadrants of the detector. Moreover, unexpected displacement or tilting of the phase-modulated beam can be monitored with another dual-quadrant photo-detector (PD₁ in Fig. 1) and corrections may be applied to the input beam or the error signal accordingly for further RAM reduction. As for the PDH scheme, to suppress RAM is not a trivial work [22]; therefore, our proposed scheme should be a promising alternative to the PDH one in applications where RAM noise suppression to lower levels may be demanded [10, 11].

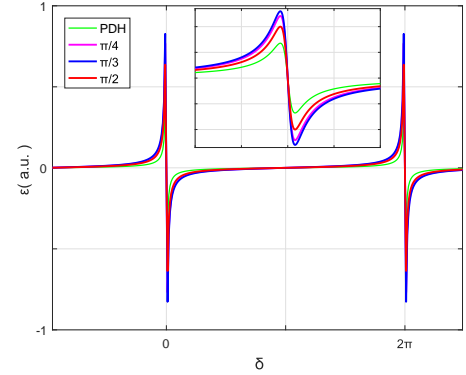


FIG. 3. (color online) Error signals for cavity locking as a function of the cavity detuning δ in comparison with that of the PDH scheme. From the simulation results, it follows that the error signal is near its maximum when $\varphi_0 = \pi/3$ (blue curve) and its size is 1.9 times that of the PDH error signal for the modulation depth of 1.08 (green curve). In the simulation, $R_1 = 99.999\%$ and $R_2 = 1$ are assumed. Moreover, the total area of S_1 and S_2 on the SOM covers half of the cross section of the incident beam.

In the preceding analysis, it was assumed that $|\varphi(\vec{r})| \ll 1$, which is nonetheless usually invalid in practice when large error signal sizes are desired. In the following, let relax this assumption and discuss how to implement cavity locking by spatial modulation of optical phase front. To that end, Eq. (2) may be replaced by

$$E_m(\vec{r}, t) = A E_1(\vec{r}, t) + E_e(\vec{r}, t), \quad (15)$$

wherein the effective field now becomes

$$E_e(\vec{r}, t) = \left[e^{i\varphi(\vec{r})} - A \right] E_i(\vec{r}, t). \quad (16)$$

Here the constant coefficient A is defined as

$$A \equiv \frac{\iint d\vec{r} \cos \varphi(\vec{r}) |E_i(\vec{r}, t)|^2}{\iint d\vec{r} |E_i(\vec{r}, t)|^2}, \quad (17)$$

which ensures the orthogonality between the effective field $E_e(\vec{r}, t)$ and the incident field $E_i(\vec{r}, t)$

$$\iint d\vec{r} E_i^*(\vec{r}, t) E_e(\vec{r}, t) = 0, \quad (18)$$

as long as the anti-symmetry (7) of the phase modulation function holds valid. Then after reflection from the cavity, the modulated light field becomes [12]

$$\begin{aligned} E_r(\vec{r}, t) &= \left\{ \sqrt{R_1} e^{i\varphi(\vec{r})} - A \frac{T_1}{\sqrt{R_1}} \frac{e^{i\delta} \sqrt{R}}{1 - e^{i\delta} \sqrt{R}} \right\} E_i(\vec{r}, t) \\ &\equiv [\chi e^{i\theta} + i \sin \varphi(\vec{r})] \sqrt{R_1} E_i(\vec{r}, t), \end{aligned} \quad (19)$$

in which

$$\chi e^{i\theta} \equiv \cos \varphi(\vec{r}) - A \frac{T_1}{R_1} \frac{e^{i\delta} \sqrt{R}}{1 - e^{i\delta} \sqrt{R}}. \quad (20)$$

After substituting Eqs. (19) and (8) into Eq. (9), one arrives at

$$\begin{aligned} \varepsilon(\delta) &= \iint_{S_1} d\vec{r} R_1 |(\chi e^{i\theta} + i \sin \varphi_0) E_i(\vec{r}, t)|^2 \\ &\quad - \iint_{S_2} d\vec{r} R_1 |(\chi e^{i\theta} - i \sin \varphi_0) E_i(\vec{r}, t)|^2 \\ &= 4R_1 I_0 \sin \varphi_0 \operatorname{Im} \left(\cos \varphi_0 - A \frac{T_1}{R_1} \frac{e^{i\delta} \sqrt{R}}{1 - e^{i\delta} \sqrt{R}} \right) \end{aligned} \quad (21)$$

from which it follows that the error signal for cavity locking varies as the cavity detunes from its peak resonance (Fig. 3) when $\sin \varphi_0 \neq 0$.

From Fig. 3 it follows that the size of the error signal can be almost twice that of the PDH one with optimized modulation depth of $\beta = 1.08$, for which the PDH scheme needs to pay the price of high-order harmonic r.f. modulation side-bands in the optical spectrum of the incident beam. We stress that the error signal in this scheme is generated as the differential photo-current from the two quadrants of the detector and, thereby, low-frequency optical and detection noises can be substantially suppressed. Despite this, the error signal may still be contaminated by residual low-frequency noises. For cases where these low-frequency noises are detrimental to laser stability, a possible solution could be to use a dual-frequency incident light field with two equal-strength components such that the error signal is up-shifted to r.f. bands. When both optical frequency components are

chosen to simultaneously resonate in the cavity, the r.f. error signal reads

$$\begin{aligned} \varepsilon(\delta) &= 4R_1 I_{AC} \sin \varphi_0 \chi \sin \theta \\ &= 4R_1 I_{AC} \sin \varphi_0 \operatorname{Im} \left(\cos \varphi_0 - A \frac{T_1}{R_1} \frac{e^{i\delta} \sqrt{R}}{1 - e^{i\delta} \sqrt{R}} \right) \end{aligned} \quad (22)$$

wherein $I_{AC} = \bar{I} \cos \Omega t$ with \bar{I} being the average power of the incident beam and Ω the optical frequency span between the two frequency components. A dual-frequency light beam may be created by a dual-frequency laser [25] or by use of an acousto-optic modulator and a single-frequency laser [26].

Last but not least, let discuss the differences between the studied cavity locking method and the tilt-locking one, the latter of which is modulation free [13]. By slightly tilting or laterally displacing the input beam of a well-aligned and mode-matched cavity, a TEM₁₀ mode may be generated to interfere with the fundamental TEM₀₀ mode to produce an error signal. This particular way to create error signal makes the system very sensitive to light beam drifting noises as evidenced by the fact that unexpected beam drifting is indistinguishable from deliberate beam alignment for error signal generation; therefore, double pass configuration with travelling-wave cavities must be used to suppress these noises [23]. This leads to the major disadvantage of the tilt-locking scheme, i.e., its incompatibility with the standing-wave cavity configuration used by the PDH method. On the contrary, spatial phase modulation in the studied method produces the error signal in a different way and hence is not so sensitive to beam drifting as the tilt locking one; in addition, residual beam drifting noises can be further corrected as discussed in the previous text. Therefore, our proposed scheme needs not stick to travelling-wave cavities and allows one to implement laser stabilization with FP cavities, just as the PDH scheme does. In other words, both the techniques of spatial modulation (our method) and temporal modulation (the PDH one) of optical phase front can share the same optical platform for laser stabilization, which will save much time and man power for cavity design.

To conclude, we have studied optical cavity locking for laser stabilization through spatial modulation of the phase front of an optical carrier. A theoretical description of the underlying principle has been developed for the cavity locking method with a special attention paid to RAM noises caused by experimental imperfections. While the studied method has the common advantages of the PDH method and the tilt-locking one, it can provide a more artful way to eliminate RAM noise in phase modulation. This method can implement laser stabilization with FP cavities like the PDH one, but giving larger error signals and cleaner spectra for the carriers than the later. In situations where cost and portability are a practical issue, the studied scheme allows one to realize laser stabilization in the PDH optical platform without use of expensive and bulky devices such as signal generators

and electro-optic modulators.

Funding This work was supported by the National Natural Science Foundation of China (12074110).

Disclosures The authors declare no conflicts of interest.

Data availability Data underlying the results presented in this paper are not publicly available at this time but may be obtained from the authors upon reasonable request.

-
- [1] N. Hinkley, J. A. Sherman, N. B. Phillips, M. Schioppa, N. D. Lemke, K. Beloy, M. Pizzocaro, C. W. Oates, and A. D. Ludlow, “An Atomic Clock with 10^{-18} Instability,” *Science* **341**, 1215–1218 (2013).
- [2] B. J. Bloom, T. L. Nicholson, J. R. Williams, S. L. Campbell, M. Bishof, X. Zhang, W. Zhang, S. L. Bromley, and J. Ye, “An optical lattice clock with accuracy and stability at the 10^{-18} level,” *Nature* **506**, 71–75 (2014).
- [3] A. D. Ludlow, M. M. Boyd, J. Ye, E. Peik, and P. O. Schmidt, “Optical atomic clocks,” *Rev. Mod. Phys.* **87**, 637–701 (2015).
- [4] C. Eisele, A. Nevsky, and S. Schiller, “Laboratory test of the isotropy of light propagation at the 10^{-17} level,” *Phys. Rev. Lett.* **103**, 090401 (2009).
- [5] E. Wiens, A. Y. Nevsky, and S. Schiller, “Resonator with Ultrahigh Length Stability as a Probe for Equivalence-Principle-Violating Physics,” *Phys. Rev. Lett.* **117**, 271102 (2016).
- [6] LIGO Scientific Collaboration, “LIGO: the laser interferometer gravitational-wave observatory,” *Rep. Prog. Phys.* **72**, 076901 (2009).
- [7] T. Fortier, M. Kirchner, F. Quinlan, J. Taylor, J. C. Bergquist, T. Rosenband, N. Lemke, A. Ludlow, Y. Y. Jiang, C. W. Oates, and S. A. Diddams, “Generation of ultrastable microwaves via optical frequency division,” *Nat. Photonics* **5**, 425–429 (2011).
- [8] D. G. Matei, T. Legero, S. Hafner, C. Grebing, R. Weyrich, W. Zhang, L. Sonderhouse, J. M. Robinson, J. Ye, F. Riehle, and U. Sterr, “1.5 μm Lasers with Sub-10 mHz Linewidth,” *Phys. Rev. Lett.* **118**, 263202 (2017).
- [9] J. M. Robinson, E. Oelker, W. R. Milner, W. Zhang, T. Legero, D. G. Matei, F. Riehle, U. Sterr, and J. Ye, “Crystalline optical cavity at 4 K with thermal-noise-limited instability and ultralow drift,” *Optica* **6**, 240–243 (2019).
- [10] J. Davila-Rodriguez, F. N. Baynes, A. D. Ludlow, T. M. Fortier, H. Leopardi, S. A. Diddams, and F. Quinlan, “Compact, thermal-noise-limited reference cavity for ultra-low-noise microwave generation,” *Opt. Lett.* **42**, 1277–1280 (2017).
- [11] W. Zhang, L. Stern, D. Carlson, D. Bopp, Z. Newman, S. B. Kang, J. Kitching, and S. B. Papp, “Ultrannarrow Linewidth Photonic-Atomic Laser,” *Laser Photonics Rev.* **14**, 1900293 (2020).
- [12] T. W. Hänsch and B. Couillaud, “Laser frequency stabilization by polarization spectroscopy of a reflecting reference cavity,” *Opt. Comm.* **35**, 441–444 (1980).
- [13] D. A. Shaddock, B. C. Buchler, W. P. Bowen, M. B. Gray, and P. K. Lam, “Modulation-free control of a continuous-wave second-harmonic generator,” *J. Opt. A* **2**, 400–404 (2000).
- [14] J. I. Thorpe, K. Numata, and J. Livas, “Laser frequency stabilization and control through offset sideband locking to optical cavities,” *Opt. Express* **16**, 15980–15990 (2008).
- [15] P. Yang and S. Feng, “Fabry-Perot cavity locking with phase-locked frequency-synthesized light,” *J. Opt. Soc. Am. B* **34**, 533–537 (2017).
- [16] H. M. Wang, Z. S. Xu, S. C. Ma, M. H. Cai, S. H. You, and H. P. Liu, “Artificial modulation-free Pound-Drever-Hall method for laser frequency stabilization,” *Opt. Lett.* **44**, 5816–5819 (2019).
- [17] R. W. P. Drever, J. L. Hall, F. V. Kowalski, J. Hough, G. M. Ford, A. J. Munley, and H. Ward, “Laser phase and frequency stabilization using an optical resonator,” *Appl. Phys. B* **31**, 97–105 (1983).
- [18] N. C. Wong and J. L. Hall, “Servo control of amplitude modulation in frequency-modulation spectroscopy: demonstration of shot-noise-limited detection,” *J. Opt. Soc. Am. B* **2**, 1527–1533 (1985).
- [19] H. Muller, S. Herrmann, T. Schuldt, M. Scholz, E. Kovalchuk, and A. Peters, “Offset compensation by use of amplitude-modulated sidebands in optical frequency standards,” *Opt. Lett.* **28**, 2186–2188 (2003).
- [20] F. Du Burck, O. Lopez, and A. El Basri, “Narrow-band correction of the residual amplitude modulation in frequency-modulation spectroscopy,” *IEEE Trans. Instrum. Meas.* **52**, 288–291 (2003).
- [21] L. Li, F. Liu, C. Wang, and L. Chen, “Measurement and control of residual amplitude modulation in optical phase modulation,” *Rev. Sci. Instrum.* **83**, 043111 (2012).
- [22] W. Zhang, M. J. Martin, C. Benko, J. L. Hall, J. Ye, C. Hagemann, T. Legero, U. Sterr, F. Riehle, and G. D. Cole, “Reduction of residual amplitude modulation to 1×10^{-6} for frequency modulation and laser stabilization,” *Opt. Lett.* **39**, 1980–1983 (2014).
- [23] N. Chhabra, A. R. Wade, E. R. Rees, A. J. Sutton, A. Stochino, R. L. Ward, D. A. Shaddock, and K. McKenzie, “High stability laser locking to an optical cavity using tilt locking,” *Opt. Lett.* **46**, 3199–3202 (2021).
- [24] A. E. Siegman, “*Laser*,” (University Science Books, 1986).
- [25] C. Chou, K.-H. Chiang, K.-Y. Liao, Y.-F. Chang, and C. Lin, “Polarized Photon-Pairs Heterodyne Polarimetry for Ultrasensitive Optical Activity Detection of a Chiral Medium,” *J. Phys. Chem. B* **111**, 9919–9922 (2007).
- [26] P. Yang, B. Y. Xie, and S. Feng, “Subhertz interferometry at the quantum noise limit,” *Opt. Lett.* **44**, 2366–2369 (2019).